

# The Iroquois homeobox proteins IRX3 and IRX5 have distinct roles in Wilms tumour development and human nephrogenesis

Linda Holmquist Mengelbier<sup>1\*</sup>, Simon Lindell-Munther<sup>1</sup>, Hiroaki Yasui<sup>1,2</sup>, Caroline Jansson<sup>1</sup>, Javanshir Esfandyari<sup>3</sup>, Jenny Karlsson<sup>1</sup>, Kimberly Lau<sup>4</sup>, Chi-chung Hui<sup>4,5</sup>, Daniel Bexell<sup>3</sup>, Sevan Hopyan<sup>4,5</sup> and David Gisselsson<sup>1,6,7</sup>

<sup>1</sup> Division of Clinical Genetics, Department of Laboratory Medicine, Lund University, Lund, Sweden

<sup>2</sup> Department of Obstetrics and Gynecology, Graduate School of Medicine, Nagoya University, Nagoya, Japan

<sup>3</sup> Division of Translational Cancer Research, Department of Laboratory Medicine, Lund University, Lund, Sweden

<sup>4</sup> Program in Developmental and Stem Cell Biology, Research Institute, The Hospital for Sick Children, Toronto, ON, Canada

<sup>5</sup> Department of Molecular Genetics, University of Toronto, Toronto, ON, Canada

<sup>6</sup> Department of Pathology, Laboratory Medicine, Medical Services, University Hospital, Lund, Sweden

<sup>7</sup> Division of Oncology and Pathology, Department of Clinical Sciences, Lund University, Lund, Sweden

\*Correspondence to: L Holmquist Mengelbier, Division of Clinical Genetics, Department of Laboratory Medicine, Lund University, BMC C13, SE22184 Lund, Sweden. E-mail: linda.holmquist\_mengelbier@med.lu.se

## Abstract

Wilms tumour is a paediatric malignancy with features of halted kidney development. Here, we demonstrate that the Iroquois homeobox genes *IRX3* and *IRX5* are essential for mammalian nephrogenesis and govern the differentiation of Wilms tumour. Knock-out *Irx3<sup>-/-</sup>/Irx5<sup>-/-</sup>* mice showed a strongly reduced embryonic nephron formation. In human foetal kidney and Wilms tumour, *IRX5* expression was already activated in early proliferative blastema, whereas *IRX3* protein levels peaked at tubular differentiation. Accordingly, an orthotopic xenograft mouse model of Wilms tumour showed that *IRX3<sup>-/-</sup>* cells formed bulky renal tumours dominated by immature mesenchyme and active canonical WNT/ $\beta$ -catenin-signalling. In contrast, *IRX5<sup>-/-</sup>* cells displayed activation of Hippo and non-canonical WNT-signalling and generated small tumours with abundant tubulogenesis. Our findings suggest that promotion of *IRX3* signalling or inhibition of *IRX5* signalling could be a route towards differentiation therapy for Wilms tumour, in which WNT5A is a candidate molecule for enforced tubular maturation.

© 2018 The Authors. *The Journal of Pathology* published by John Wiley & Sons Ltd on behalf of Pathological Society of Great Britain and Ireland.

**Keywords:** Wilms tumour; Iroquois; IRX3; IRX5; nephrogenesis; differentiation; WNT5A

Received 6 July 2018; Revised 27 August 2018; Accepted 16 September 2018

No conflicts of interest were declared.

## Introduction

Wilms tumour is the most common renal neoplasm in children. Its biology and morphology closely mirror the early stages of mammalian kidney development (nephrogenesis). A key element of nephrogenesis is the transformation of the blastemal elements of the metanephric mesenchyme, via mesenchymal-to-epithelial transition (MET), into the functional units of the kidney, the nephrons. MET is initiated by reciprocal induction between the ureteric bud (UB) and the blastema, followed by polarisation and differentiation of the blastema via gradually maturing epithelial structures, such as renal vesicles, comma-shaped bodies (CSB) and S-shaped bodies (SSB), that ultimately form tubules and glomeruli [1]. Wilms tumours result from a disturbance of these processes with the accumulation of cells that retain features of the immature metanephric mesenchyme/blastema, with a variable degree of differentiation towards

epithelial and stromal elements. This explains the tumour's classic triphasic histology. Tumours with a predominance of blastemal cells after treatment are associated with inferior prognosis, as are tumours with regions harbouring pleomorphic and disorganised cells, a feature referred to as diffuse anaplasia [2]. Wilms tumour patients currently have an overall survival rate approaching 90%, but this comes at the price of heavy chemotherapy, often resulting in severe and/or life-long side effects [3,4]. Identification of agents that could induce differentiation of Wilms tumour cells into nephrogenic structures could be a future route towards reducing cytotoxic treatment.

Somatic mutations and chromosomal rearrangements have been associated with high-risk histological features and inferior outcome in Wilms tumour patients. Among those are hemizygous deletions in chromosome arm 16q [5]. The smallest region of genomic overlap between these deletions has been shown to harbour the Iroquois homeobox B (IRXB) gene cluster, consisting of *IRX3*,

*IRX5* and *IRX6* [6]. *IRX3* and *IRX5* encode proteins that have recently been shown to be essential for several aspects of embryogenesis, such as the development of the nervous system, heart and skeleton [7–11]. The Iroquois genes *Irx3* and *Irx5* are both expressed in the developing mouse kidney [12], but so far, no specific function for *Irx5* in nephrogenesis has been reported [13]. *Irx3*, on the other hand, has been shown to be important in nephron formation and segmentation in both *Xenopus* and zebrafish [14–16]. This background encouraged us to further study the roles of *IRX3* and *IRX5* in Wilms tumour and kidney development with the ultimate purpose of identifying signalling pathways that could be manipulated for the induction of Wilms tumour differentiation.

## Materials and methods

### Mouse models, patient material and human cell lines

One wild type (*wt*), four *Irx3/Irx5*<sup>+/-</sup> and four *Irx3/Irx5*<sup>-/-</sup> E13.5 foetal mouse kidneys were available for analysis [11]. Mouse experiments were performed following ethics permit ‘Mouse Limb Development’ #33868 (Mouse) approval by the Hospital for Sick Children Animal Care Committee, Toronto, Canada. Use of patient material was approved by the Regional Ethics Review Board with approval reference numbers L605-2005 (biobanking), L289-2011 (molecular analyses of tumours) and L796-2017 (analysis of anonymised post-mortem material), according to the Helsinki Declaration of 1975, as revised in 1983. Material from 39 primary Wilms tumours, two anonymised postnatal kidneys and five anonymised foetal kidneys were analysed (see supplementary material, Table S1). The Wilms tumour WiT49 cell line, kindly provided by Dr. Yeger at the Laboratory of Medicine and Pathobiology, University of Toronto, Canada [17], has been repeatedly characterised by our lab [18,19]. WiT49 cells were used to create *IRX3* and *IRX5* knockout cells through targeted genome editing to create *IRX3*<sup>-/-</sup> and *IRX5*<sup>-/-</sup> cells as detailed in the supplementary material, Supplementary materials and methods and Table S2. *In vitro*, cells were cultured in DMEM F:12 1:1 supplemented with 10% foetal bovine serum and 1% penicillin–streptomycin.

### Orthotopic xenograft transplantation and magnetic resonance imaging

One million WiT49 wild-type, *IRX3*<sup>-/-</sup> or *IRX5*<sup>-/-</sup> cells in 20 µl PBS were injected into the left kidney of female NSG mice (4–6 weeks old; Charles River Laboratories, Wilmington, MA, USA) as described previously [19]. Thirteen mice were injected with WiT49 wild-type cells, 14 with *IRX3*<sup>-/-</sup> cells and 9 with *IRX5*<sup>-/-</sup> cells (see supplementary material, Table S3). Magnetic resonance imaging (MRI) was performed 12 weeks after tumour cell injection as described previously (9.4 T horizontal

bore, Lund University Bioimaging Center, Sweden; [20]). MRIs were scrutinised using the Sante DICOM viewer 3D (Santesoft, Nicosia, Cyprus). Tumour volumes were calculated using the DICOM viewer software OsiriX (Pixmeo SARL, Switzerland). Volume was registered as 0 if no tumour was visible or if rendered immeasurable by being present in one MRI section only (see supplementary material, Table S3). Mice were sacrificed 3 months after xenotransplantation. Xenograft animal studies were performed according to ethics permit M11-15 (Malmö-Lund Animal Research Ethics Committee, Lund, Sweden).

### Immunohistochemistry and histological imaging

Paraffin-embedded tissue was deparaffinised and prepared for immunohistochemistry (IHC) according to standard procedures. Details about antibodies, their working solutions and procedures can be found in supplementary material, Table S4 and Supplementary materials and methods. Slides subjected to IHC or haematoxylin and eosin (H&E) staining were scanned using an Aperio ImageScope v12.1.0.5029 (Leica Biosystems, Wetzlar, Germany) or photographed with a digital SC50 camera (Olympus, Tokyo, Japan).

For murine embryonic kidneys, UB-derived CALB1-positive structures were distinguished from N-cadherin-positive CSB and SSB, while E-cadherin was used to identify all epithelial foetal kidney components. CALB1-immunostained sections were compared to consecutive sections stained for E-cadherin to confirm the classification of CSB and SSB as opposed to UB-derived structures. The total number (*n*) of CALB1- and N-cadherin-stained sections available for analysis in each group was: wild type: *n* = 3; *Irx3/Irx5*<sup>+/-</sup>: *n* = 14; and *Irx3/Irx5*<sup>-/-</sup>: *n* = 8. The Wilcoxon rank-sum test was used for significance tests. For analysis of clinical Wilms tumour samples, a tissue microarray (TMA) with cores from 33 primary tumours was used for the evaluation of *IRX3* and *IRX5* protein expression [21]. *IRX3* and *IRX5* were categorised as present or absent (see supplementary material, Table S1).

Xenograft Wilms tumours were evaluated for the percentage of tumour surface area consisting of neoplastic tubules. Positive WT1 expression identified tubular epithelial cells, whereas p53 positivity was used for demarcation of tumour borders in contrast to host mouse kidney tissue (see supplementary material, Figure S1). Thirteen wild-type WiT49 tumours, 12 *IRX3*<sup>-/-</sup> tumours [C2 (*n* = 6) and T5\_40 (*n* = 6)] and 7 *IRX5*<sup>-/-</sup> tumours [T5\_34 (*n* = 2), T5\_71 (*n* = 3) and T5\_77 (*n* = 2)] provided sufficient tumour material for analysis (see supplementary material, Table S3). Evaluation of WNT5A expression was performed on sections from four WiT49 wild-type, six *IRX3*<sup>-/-</sup> and two *IRX5*<sup>-/-</sup> xenograft tumours (see supplementary material, Table S3). All tumour areas containing stroma were digitalised, and all stroma cells [wild type (*n* = 3054 cells), *IRX3*<sup>-/-</sup> (*n* = 5010 cells) and *IRX5*<sup>-/-</sup> (*n* = 1115 cells)] were scored as positive or negative for WNT5A

protein expression. Fisher's exact test (two-sided) was used to evaluate any differences between groups.

#### RNA and protein extraction and gene and protein expression analyses

WiT49 wild-type ( $n=5$ ), *IRX3* knockout [C2 ( $n=3$ ) and T5\_40 ( $n=3$ )] and *IRX5* knockout (one each of T5\_34, T5\_71, T5\_77, T5\_56 and T5\_110) cells were seeded and grown for 48 h. Biological replicates were grown for WiT49, C2 and T5\_40 in order to increase the number of samples for statistical analysis. For global gene expression analyses, whole transcriptome RNA sequencing was performed on an Ion Ampliseq (Thermo Fisher Scientific, Waltham, MA, USA) at the National Genomics Infrastructure, SciLife Uppsala Core Facility, Uppsala, Sweden. To explore active signalling pathways in *IRX3*<sup>-/-</sup> and *IRX5*<sup>-/-</sup> cells, gene expression data were analysed by Gene Set Enrichment Analysis (GSEA; [22,23]; GSEA 3.0 (<http://www.broadinstitute.org/gsea/>), Broad Institute, Cambridge, MA, USA). For targeted pathway analysis, QluCore Omics Explorer 3.2 and 3.3 (QluCore, Lund, Sweden) were used. Further details for gene expression analysis and information about protein extraction and Western blotting are provided in supplementary material, Supplementary materials and methods.

#### Cell proliferation assays

Cell proliferation assays were performed on the original WiT49 clone and its *IRX3*<sup>-/-</sup> and *IRX5*<sup>-/-</sup> clones using an MTS assay (CellTiter 96<sup>®</sup> AQueous One Solution Cell Proliferation Assay, G3582, Promega, Madison, WI, USA) and IncuCyteZoom<sup>®</sup> (Essen BioScience, Ann Arbor, MI, USA). For details, see supplementary material, Supplementary materials and methods.

## Results

### Reduced nephron morphogenesis in *Irx3/Irx5* knockout mice

To evaluate whether *Irx3* and *Irx5* influence normal mammalian kidney development, we first turned to an already established mouse model in which *Irx3* and *Irx5* had been either heterozygously or homozygously deleted [11]. Given that *Irx3* and *Irx5* show redundant functions in mouse heart development, we chose to study double-knockout embryos when probing for an effect on nephrogenesis [8,24]. *Irx3/Irx5*<sup>-/-</sup> embryos die at E13.5 due to heart failure [8,11]. Therefore, we examined nephron formation during early kidney development (E13.5) and compared mice of *wt* or in which *Irx3* and *Irx5* had been either heterozygously or homozygously deleted (Figure 1). N-cadherin immunostaining was used to identify cells and structures destined to become parts of proximal tubules, including SSB and CSB. Compared to *wt* and *Irx3/5*<sup>+/-</sup> mice,

maturing nephrogenic epithelial elements were close to absent in *Irx3/Irx5*<sup>-/-</sup> mice (Figure 1M–R). CSB and SSB were significantly more prevalent in *wt* compared to *Irx3/Irx5*<sup>+/-</sup> ( $p=0.022$ ) and *Irx3/Irx5*<sup>-/-</sup> ( $p=0.013$ ) embryonal mouse kidneys (Wilcoxon rank-sum test, Figure 1S). This role for *Irx3/Irx5* in murine nephron formation encouraged further delineation of IRX3 and IRX5 in a context of human nephrogenesis and Wilms tumour.

### IRX3 and IRX5 are expressed in distinct tissue elements of foetal kidney and Wilms tumour

In human foetal kidney specimens (Figure 2), the nephrogenic epithelium was IRX3-positive by IHC, whereas UB-derived structures were negative (Figure 2A–C). Primitive nephrogenic structures of the nephrogenic zone, such as renal vesicles, CSB and SSB, as well as mature proximal tubules were IRX3-positive (Figure 2D–F). The expression of IRX3 in cap mesenchyme (CM) was minimal (Figure 2D,E), and its expression increased with the time of gestation (Figure 2B,J,E), subsequently decreasing in the postnatal kidney (Figure 2F,L; see supplementary material, Figure S2A–D). IRX5 showed a similar expression pattern to IRX3 but was more prominently expressed in CM, renal vesicles and early-stage nephrogenic tubules (Figure 2G,H and supplementary material, Figure S2E). IRX5 expression was retained in nephrons of postnatal normal kidney (Figure 2I). IRX3 and IRX5 showed predominantly cytoplasmic expression, with little nuclear expression at early nephrogenesis and none in postnatal kidney (Figure 2J–M). Similar to that observed in the human foetal kidney, IHC analysis of a TMA containing cores from  $\geq 30$  primary Wilms tumours demonstrated that IRX3 was expressed in the epithelial elements of almost all tumours, compared to blastemal components in a minority of cases, and in stromal components only very rarely (Figure 2N–P, T and supplementary material, Figure S2F). IRX5 was also expressed in epithelial components, but contrary to IRX3, it was also commonly expressed in blastemal and stromal elements (Figure 2Q–T). The IRX3 and IRX5 proteins were detected in both nucleus and cytoplasm (Figure 2N–S). Taken together, these results indicated that IRX3 may play a role primarily during maturation of nephrogenic elements, while IRX5 activity is also present in the stromal and proliferative late blastemal/early epithelial cells in developing kidneys and Wilms tumours.

### IRX3 and IRX5 knockout Wilms tumour cells have contrasting phenotypes *in vitro*

To elucidate the functionality of IRX3 and IRX5 in Wilms tumour development, targeted genome editing of *IRX3* and *IRX5* was performed on the human WiT49 Wilms tumour cell line, chosen as a model system as it retains the multi-phasic histology of Wilms tumours when orthotopically xenografted into mice [17,19,25,26]. Most importantly, the model enables the

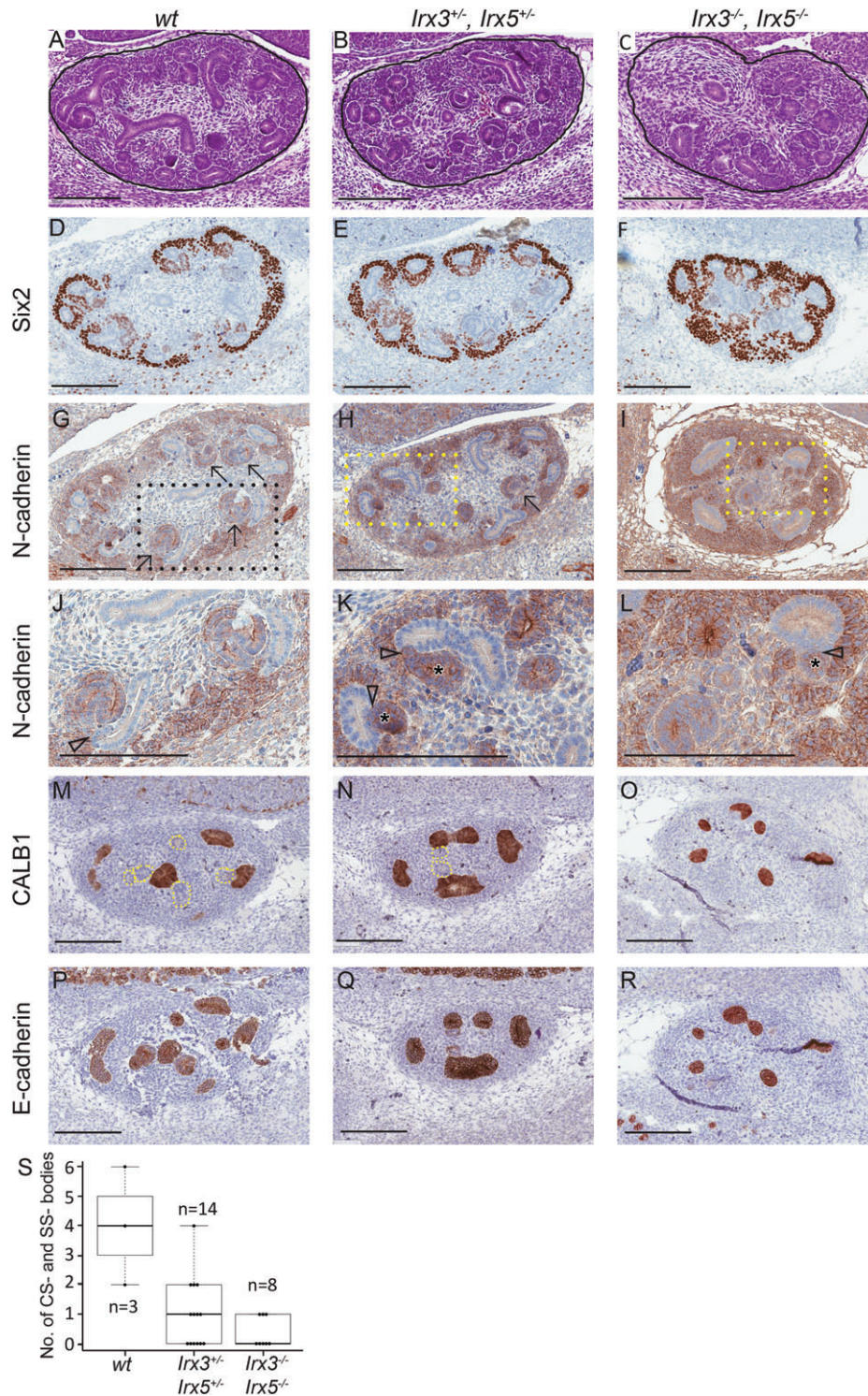


**Figure 1.** Reduced nephron morphogenesis in *lrx3/lrx5* knockout mice. Representative images of *lrx3* and *lrx5* wt, heterozygous and homozygous knockout E13.5 foetal mouse kidney (FMK) sections stained with H&E (Htx; A–C). The CM/committed blastema, identified by Six2 expression was retained in all genotypes (D–F), although it was more extensively manifested in homozygous (*lrx3*<sup>-/-</sup> *lrx5*<sup>-/-</sup>) mice (F). *lrx3/5*<sup>-/-</sup> mice, as opposed to wt and heterozygous mice, showed N-cadherin positivity largely confined to cells of the CM as if differentiation through CSB and SSB had ceased (G–L). Specific labelling of UB structures with CALB1 (M–O), in combination with staining for all epithelial elements in the foetal kidney by E-cadherin (P–R), confirmed that almost all epithelial structures were UB-derived in *lrx3/5*<sup>-/-</sup> mice (O and R). *lrx3/lrx5* knockout mice maintained the ability to form some primitive nephrogenic tubules with a distinct lumen and could dock to UB-derived structures, but the tails of the SSB were consistently missing in *lrx3/lrx5* hetero- and homozygous knockout embryos, resulting in short tubules without curvature (K and L). Solid black lines demarcate the developing kidney from surrounding tissue (A–C). Arrows point to CSB and SSB in G and H. Content in rectangles with dashed lines in G–I are enlarged in J–L. Arrowheads point at docking sites between nephrogenic and UB-derived epithelial structures, and asterisks (\*) denote the lumen of nephrogenic tubules in K–L. Dotted lines in M and N correspond to E-cadherin-positive structures in P and Q. Scale bars correspond to 200 µm. All immunostains are brown. Box plot showing the median number and quartiles of CSB and SSB in FMK (S), where n denote the number of sections analysed for CSB and SCB in each group.

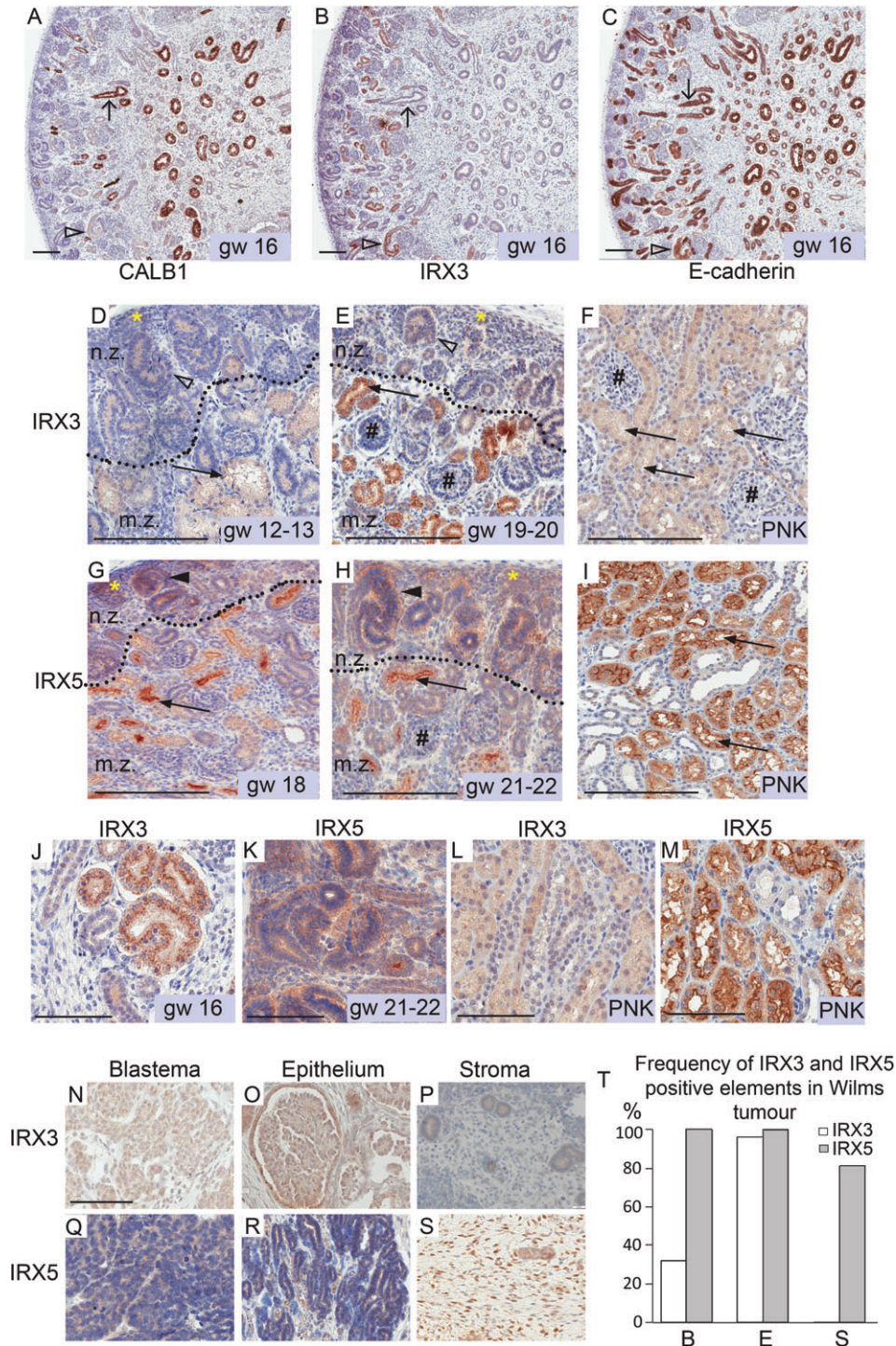


**Figure 2.** IRX3 and IRX5 are expressed in nephrogenic elements of human foetal kidney and distinct compartments of Wilms tumours. Expression of IRX3 and IRX5 proteins in human foetal and postnatal kidneys were identified by IHC. Consecutive sections of human kidney, at gestational week (gw) 16, were immunostained for CALB1 (A), IRX3 (B) and E-cadherin (C). E-cadherin was used for the detection of all epithelial structures of the kidney, and UB-derived structures were characterised by CALB1 expression. Arrows with open heads point at CALB1-positive/UB-derived epithelial elements negative for IRX3. Open arrowheads point at IRX3 and E-cadherin-positive nephrogenic structures, which are negative for CALB1. IRX3- (D, E) and IRX5 (G, H)-positive elements in human foetal (D, E and G, H) and postnatal kidney (PNK; F, I). Magnification of previous figures to illustrate cytoplasmic staining of IRX3 and IRX5, where scale bars correspond to 100  $\mu$ m (J–M). Dotted lines indicate a border between the immature subcapsular nephrogenic zone (n.z.) and the more mature central zone (m.z.) of the developing kidney. Yellow asterisks denote cap/metanephric mesenchyme. Arrows point at the ruffled lumen of proximal tubules. Open arrowheads point at IRX3-positive CSB and SSB. Filled arrowheads in G–H denote IRX5-positive CSB and SSB. IRX3- (E, F) and IRX5 (H)-negative glomeruli are denoted by hash (#). Scale bars correspond to 200  $\mu$ m. N–S: IRX3 and IRX5 protein expression evaluated by IHC in Wilms tumour (WT) histological sub-compartments from which representative areas are shown (N–P and Q–S, respectively). Scale bars correspond to 100  $\mu$ m. All immunostains are brown. (T) Bar chart summarising the frequency of IRX3- and IRX5-positive blastemal (B), epithelial (E) and stromal (S) elements in primary Wilms tumours based on examination of a WT TMA (IRX3,  $n = 33$  primary WTs; IRX5,  $n = 30$  primary WTs; Table S1).

evaluation of tumour tubule formation, corresponding to Wilms tumour epithelial differentiation. Two *IRX3* and five *IRX5* knockout clones were successfully created (see supplementary material, Figure S3, Table S2). Attempts were made for the generation of *IRX3/IRX5* double-knockout clones, but these were unsuccessful. *In vitro*, there were clear morphological differences between the knockout cell lines (see supplementary material, Figure S4A–F), with *IRX5*<sup>-/-</sup> cells growing in epithelial monolayers, while *IRX3*<sup>-/-</sup> and *wt* cells had a fibroblast-like appearance and formed tumour spherules. *IRX5*<sup>-/-</sup> knockout clones showed decreased proliferation by two independent methods compared to *WT49* and *IRX3*<sup>-/-</sup> cells (see supplementary material, Figure S5). RNA sequencing of cultured cells (see supplementary material, Table S5), followed by GSEA, demonstrated signatures of cell cycle regulators and progenitor cell renewal in *IRX3*<sup>-/-</sup> cells (see supplementary material, Table S6A and Figure S4G). In contrast, the expression of genes involved in nephrogenic maturation, such as cell polarity, epithelial sheet formation and development, was significantly enriched for in *IRX5*<sup>-/-</sup> cells (see supplementary material, Figure S4H–J and Table S6B,C).

#### Lack of IRX3 blocks tubular maturation and promotes tumourigenesis *in vivo*

To simulate Wilms tumourigenesis *in vivo*, we performed orthotopic xenograft transplantation of  $1 \times 10^6$  *wt*, *IRX3*<sup>-/-</sup> or *IRX5*<sup>-/-</sup> *WT49* cells into the left kidney of immunodeficient NSG (NOD scid gamma) mice. MRI 12 weeks after transplantation repeatedly showed bulky tumour development from *wt* and *IRX3*<sup>-/-</sup> xenograft cells, with no difference in tumour size between the genotypes (Figures 3A,B and 4A;  $p = 0.56$ , Wilcoxon rank-sum test). The tumours were readily visible macroscopically when the mice were sacrificed at 14–15 weeks after transplantation (Figure 3D,E,G,H). Histologically, both *wt* and *IRX3*<sup>-/-</sup> xenograft tumours were dominated by a large mesenchymal/stromal compartment (Figures 3J,K and 4C–H), readily discernible from the murine host kidney cells through the endogenous accumulation of mutated p53 in *WT49* cells [17]. *Wt* and *IRX3*<sup>-/-</sup> tumours grew mostly in a sarcomatous fashion, displacing or engulfing nephrons and collecting ducts of the host kidney (Figures 3M,N and 4D,G). The areas of tumour tubules in *IRX3*<sup>-/-</sup> tumours were significantly reduced compared to those in *wt* tumours in accordance with a role for IRX3 in tubular maturation (Figure 4B,E,H;  $p = 0.0002$ , Wilcoxon rank-sum test).

#### Loss of IRX5 stimulates and maintains a differentiated state

Tumours emerging from grafted *IRX5*<sup>-/-</sup> cells were either very small or were undetectable by MRI (see supplementary material, Table S3). They were rarely visible macroscopically upon harvest (Figure 3C,F,I) and their volumes were significantly smaller than *wt* and *IRX3*<sup>-/-</sup>

tumours as measured by MRI (Figure 4A;  $p = 0.002$  and  $p = 0.009$ , respectively, Wilcoxon rank-sum test) and microscopic analysis, respectively (Figure 3L,O,R compared to Figure 3J,K,M,N,P,Q). In fact, some *IRX5*<sup>-/-</sup> tumours were only possible to ascertain after p53 and WT1 IHC (see supplementary material, Figure S6A–F). The size of the tumours indicated a low proliferation rate of *IRX5*<sup>-/-</sup> cells, which recapitulated the results shown *in vitro*. Notably, clone T5-77 also formed small tumours despite its lack of suppressed proliferation *in vitro* (Figure 4A and see supplementary material, Figure S5). *IRX5*<sup>-/-</sup> tumours were histologically dominated by the epithelium (Figures 3R and 4K and see supplementary material, Figure S6C,F), with significantly more tumour tubules compared to both *wt* and *IRX3*<sup>-/-</sup> tumours ( $p = 0.02$  and  $p = 0.0004$ , Wilcoxon rank-sum test; Figure 4B–K). Their mesenchymal/stromal compartments were minimal or absent (see supplementary material, Figure S6A–F). The two proteins did not appear to compensate for each other's expression in the xenograft knockout tumours, suggesting that other pathways downstream of the IRX proteins mediate the contrasting phenotypes (see supplementary material, Figure S6G–J).

#### IRX3 and IRX5 knockout affects WNT and Hippo signalling in different ways

To unravel the signalling pathways involved in the distinct phenotypes of *IRX3*<sup>-/-</sup> and *IRX5*<sup>-/-</sup> tumours, targeted gene expression analyses of key genes for nephrogenesis was performed [27]. Here, *IRX5*<sup>-/-</sup> cells had a signature more similar to that of *wt* *WT49* cells than to *IRX3*<sup>-/-</sup> cells (Figure 5A). This was consistent with the higher prevalence of nephrogenic tubules in *wt* and *IRX5*<sup>-/-</sup> tumours compared to that of *IRX3*<sup>-/-</sup> tumours. Both WNT and Hippo signalling are known to be involved in nephrogenesis through, for example, planar cell polarity (PCP), which is important for tubule formation [28]. Gene sets involved in both these pathways exhibited distinct expression signatures at comparison between *IRX3*<sup>-/-</sup> and *IRX5*<sup>-/-</sup> cells [Figure 5B,E; multi-group comparison by analysis of variance (ANOVA)]. WNT5A is a key player in kidney development. Besides acting via the non-canonical PCP WNT pathway [29], it can signal through the WNT receptor Fzd3 (reviewed in [30–32]). Downstream of WNT receptor Fzd3, the cell adhesion molecule Alcam acts via the non-canonical WNT/JNK pathway to affect proximal tubule development [33]. Strikingly, *WNT5A*, *FZD3* and *ALCAM* were all upregulated in *IRX5*<sup>-/-</sup> cells (Figure 5B,C). Expression data suggested that canonical  $\beta$ -catenin WNT signalling was suppressed in *IRX5*<sup>-/-</sup> cells as genes involved in inhibition of  $\beta$ -catenin (*CTNNBIP1*, *DKK3* and *KREMEN1*) were upregulated in *IRX5*<sup>-/-</sup> cells, and *CTNNB1* itself was downregulated (Figure 5B). The reverse was true for *IRX3*<sup>-/-</sup> cells (Figure 5B).

Hippo signalling is involved in the regulation of organ size, and it consists of a cascade of negative growth

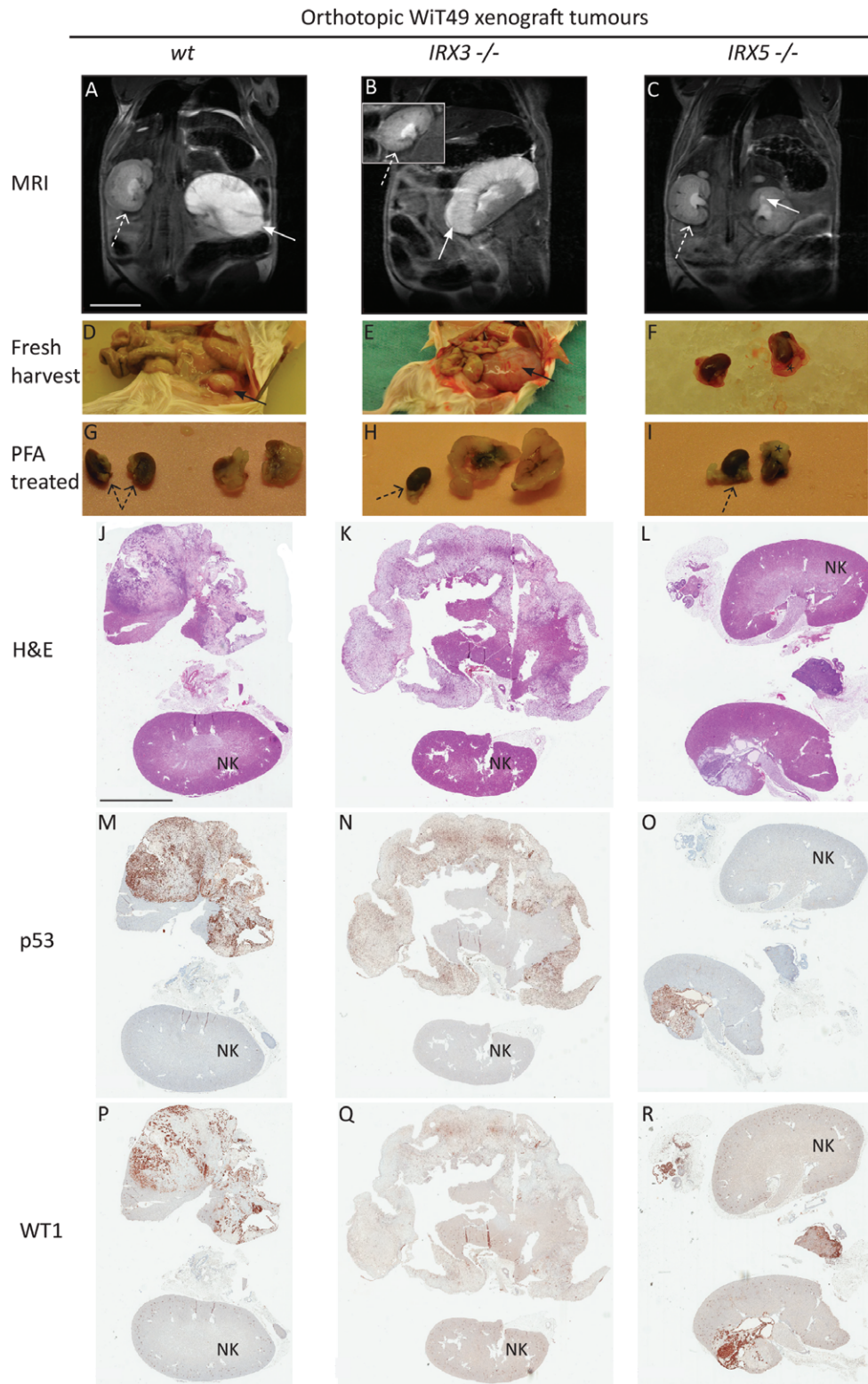


**Figure 3.** Distinct roles of *IRX3* and *IRX5* in orthotopic Wilms tumour xenografts. NSG mice were monitored by MRI 12 weeks after xenotransplantation of *wt* (A), *IRX3*<sup>-/-</sup> (B) or *IRX5*<sup>-/-</sup> (C) human Wilms tumour WiT49 cells into the left kidney. Arrows point at the tumour-afflicted left kidney (A, B, C). Dashed arrows point at the unaffected right kidney (inset in B). Tumours appear as white areas with high signal intensity. Scale bar corresponds to 1 cm. Xenograft tumours were harvested and documented approximately 14 weeks after transplantation (D–F), followed by fixation of both kidneys in paraformaldehyde (PFA, G–I). Asterisks (\*) denote visceral fat of the left kidney (F, I). Black dashed arrows point at unaffected right kidneys. Visualisation of tumour histology was carried out by H&E stains of xenograft tumours (J–L). IHC p53 positivity demonstrates tumour areas (M–O), whereas WT1 nuclear positivity enhances epithelial tumour elements (P–R). Scale bar corresponds to 5 mm. NK, normal kidney. All immunostains are brown.

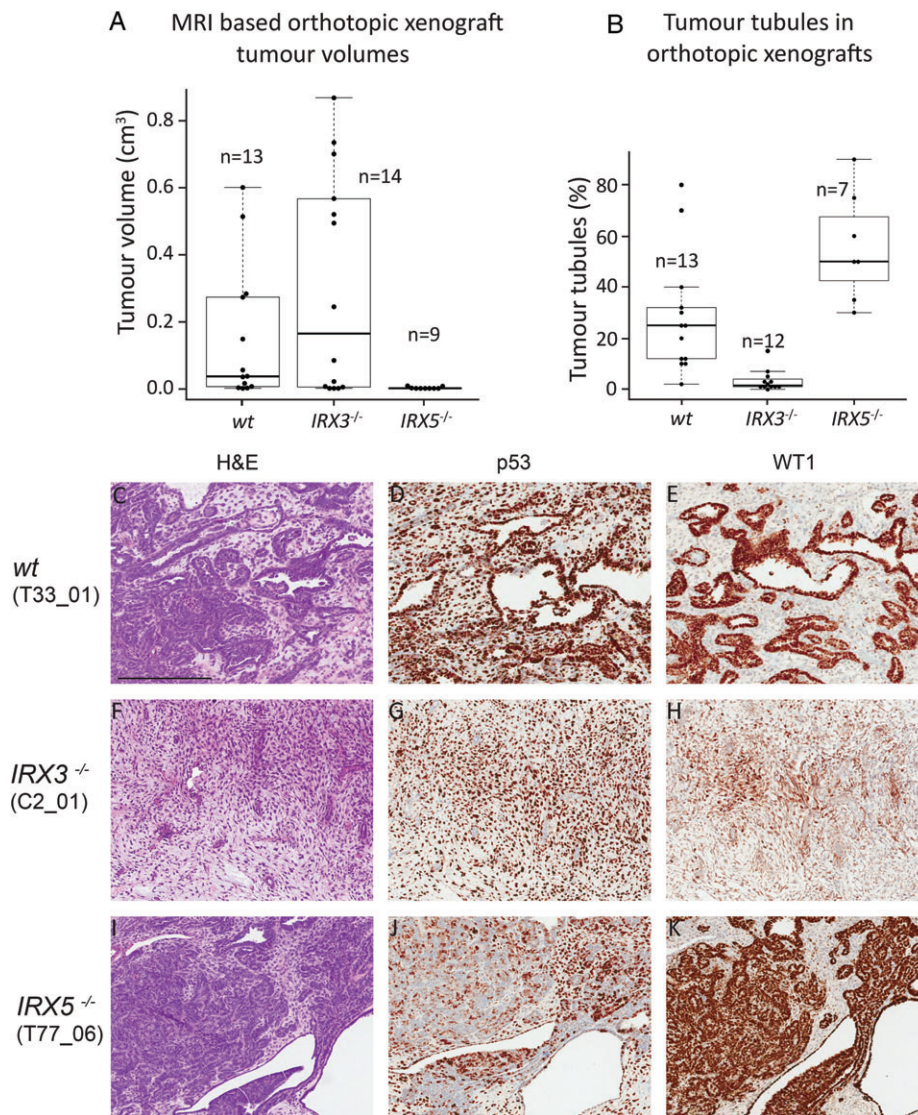


**Figure 4.** Loss of IRX3 promotes proliferative mesenchymal xenograft tumours, whereas loss of IRX5 stimulates differentiation of tumour tubules. (A) Tumour volumes based on MRI of NSG mice 12 weeks after xenograft transplantation with *wt*, *IRX3* and *IRX5* knockout orthotopic Wilms tumour xenografts. (B) The area of each tumour consisting of neoplastic tubules in *wt*, *IRX3* and *IRX5* knock out orthotopic xenografts. Boxplot represents median values and quartiles. (C–K): Detailed histological view of Wilms tumour orthotopic xenograft tumours with different IRX status, visualised by H&E staining (C, F, I) and IHC staining for p53 (D, G, J) and WT1 (E, H, K). The epithelial compartment of xenograft tumours was visualised by nuclear WT1 positivity, whereas p53 demarcated tumour cells from mouse host tissue. Within parentheses ( ) are the denotations of the specific xenograft tumours, listed in supplementary material, Table S3. Scale bar corresponds to 400 µm. All immunostains are brown.

regulators. Hence, active Hippo signalling is considered important for nephrogenesis and the suppression of tumour formation [34]. The expression of genes involved in Hippo signalling was significantly enriched in *IRX5*<sup>-/-</sup> cells (Figure 5D and see supplementary material, Table S6D). In addition, specific genes important for the activation of Hippo signalling, such as *AMOT*, *AMOTL2*, *DCHS1*, *DCHS2* and the PCP-related *FAT3* and *FAT4*, were upregulated in *IRX5*<sup>-/-</sup> cells compared to *IRX3*<sup>-/-</sup> cells (Figure 5E). Taken together, our data suggested that canonical WNT signalling was promoted in *IRX3*<sup>-/-</sup> cells, whereas Hippo and non-canonical WNT signalling were inhibited. The opposite was true for *IRX5*<sup>-/-</sup> cells (Figure 5F).

**WNT5A is a likely effector of nephrogenic tubule maturation**

WNT5A is a key effector molecule in nephrogenesis and is also integrated with Hippo signalling [29,35]. It also plays a role in tumorigenesis and has been used to enforce the differentiation of colon cancer cells [36]. *WNT5A* mRNA expression was higher in *IRX5*<sup>-/-</sup> compared to *IRX3*<sup>-/-</sup> cells (Figure 5B), while *WNT5A* protein was expressed in all histological elements of WiT49-derived tumours irrespective of *IRX3/5* status (Figure 6A–F). *WNT5A*-positive mesenchymal cells were significantly more common in *wt* and *IRX5*<sup>-/-</sup> as opposed to the poorly differentiated *IRX3*<sup>-/-</sup> tumours (Fisher’s exact test (two-sided), *p* < 0.01, supplementary material, Figure S7), in line with its lower

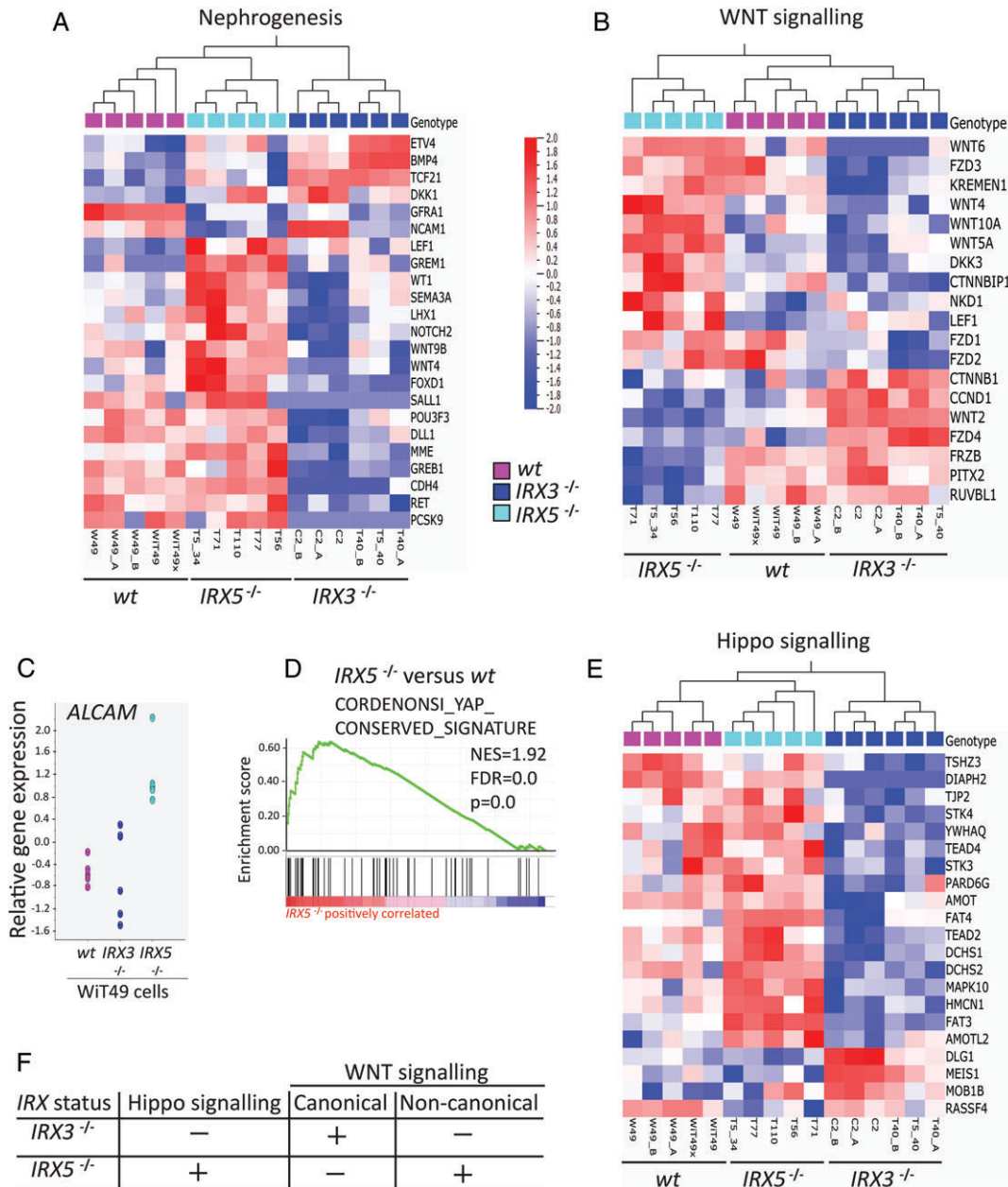
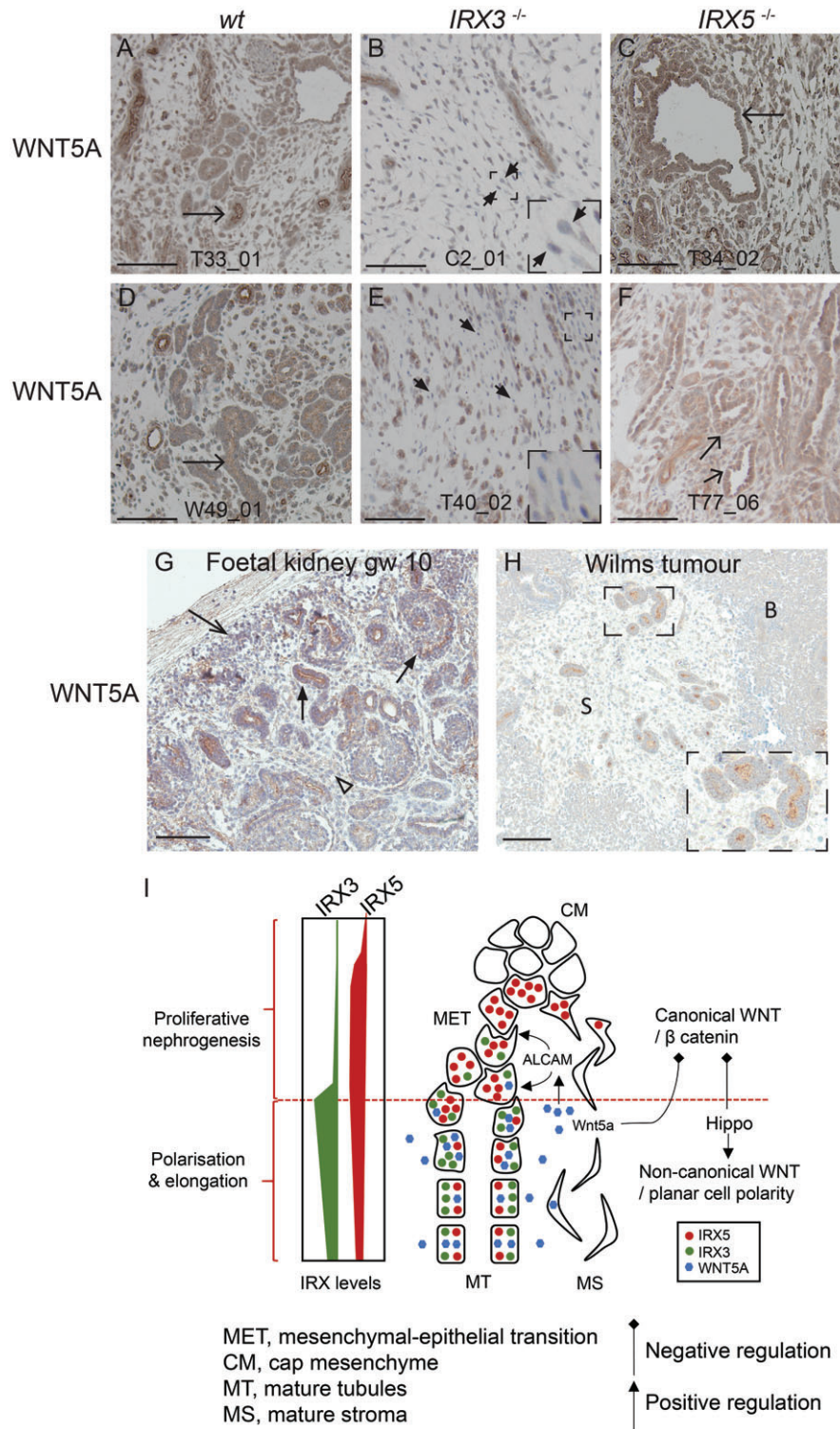


Figure 5. WNT and Hippo signalling-related genes are differentially expressed between *IRX3*- and *IRX5*-ko WiT49 cells. (A) Nephrogenesis-related genes (23/54 genes,  $p=0.02$ ) and (B) WNT signalling-related genes (19/84 genes,  $p=0.01$ ) were differentially expressed between *wt*, *IRX3*<sup>-/-</sup> and *IRX5*<sup>-/-</sup> WiT49 cells at multi-group comparison by ANOVA (false detection rate = 0.05). Extracted genes were subjected to hierarchical clustering, and results were graphically displayed as heat maps. For further details, see Materials and Methods and supplementary material, Supplementary materials and methods and Table S7. Scatter plot displaying gene expression of the key nephron tubulogenesis gene *ALCAM* (C). GSEA supported the role of Hippo signalling in *IRX5*<sup>-/-</sup> WiT49 cells. (D); GSEA run against the C6 oncogenic signatures gene sets). In addition, Hippo-related genes (21/76 genes,  $p=0.01$ , multi-group comparison by ANOVA) were differentially expressed between *wt*, *IRX3*<sup>-/-</sup> and *IRX5*<sup>-/-</sup> WiT49 cells (E). The gene expression differences between *IRX3*<sup>-/-</sup> and *IRX5*<sup>-/-</sup> cells imply that Hippo and non-canonical WNT signalling are promoted in *IRX5*<sup>-/-</sup> cells, whereas in *IRX3*<sup>-/-</sup> cells, canonical WNT signalling is activated, and Hippo signalling is inhibited (F). The heat map scale units apply to all heat maps (A, B and E).

mRNA expression in the latter. WNT5A was primarily expressed in the maturing epithelial structures of the human foetal kidney (Figure 6G). In Wilms tumours, WNT5A showed the most prominent protein expression in tumour tubular epithelium, along with areas of surrounding stromal cells (Figure 6H and supplementary material, Figure S8A–F). Blastema was repeatedly negative ( $n=6$ ; Figure 6H). Taken together, these data implicate a collaborative role of WNT5A and *IRX3* in the promotion of tumour tubulogenesis.

Discussion

Our study demonstrates that *Irx3* and *Irx5* are both expressed in primitive nephrons and regulate essential components of kidney formation in mice and humans. The expression pattern of *IRX3* suggests its involvement primarily in the maturation of human nephrogenic structures, in line with the role of the Iroquois transcription factors in the patterning of nephrogenic tubules



**Figure 6.** WNT5A is a likely differentiation-promoting agent in Wilms tumour. WNT5A detected by IHC in Wit49-based *IRX3* and *IRX5* knockout xenografts (A–F). Arrows point at WNT5A-positive tumour tubules. Short arrows point at WNT5A-negative stroma cells. Areas magnified  $\times 3$  of WNT5A-negative stroma cells are inserted in (B) and (E). WNT5A expression in human foetal kidney at gestational week (gw) 10 and Wilms tumour (G and H, respectively). Arrowhead points at WNT5A-positive stroma. Arrow with open arrowhead points at WNT5A-positive metanephric mesenchyme. Arrows with filled arrowheads denote primitive nephrogenic elements. The insertion in H is a  $\times 2$  magnification of tumour tubules (H). Scale bars correspond to 100  $\mu$ m. S = stroma. B = blastema. All immunostains are brown. (I) Cartoon depicting the proposed interplay between IRX3, IRX5 and WNT5A in nephrogenesis. IRX5 acts together with canonical/WNT- $\beta$  catenin signalling and disturbed Hippo signalling to maintain proliferative nephrogenesis. Polarisation and elongation are obtained via the integration of active Hippo and non-canonical WNT signalling, where IRX3 and WNT5A, via stimulation of ALCAM, are crucial. Disturbed IRX3 and IRX5 expression, epitomised by Wilms tumour, inhibits MET and polarisation of immature mesenchyme. According to our model, exogenous WNT5A could potentially override the differentiation block present in Wilms tumour.

in the pronephros of zebrafish and amphibians [14–16]. In contrast, the *IRX5* expression pattern indicated a role for it primarily in the maintenance of a proliferative pool of nephrogenic cells and the cells of early tubule formation. Apart from our study, the evidence for a role of *Irx5* in nephrogenesis is sparse [12]. In accordance with the distinct roles of the two proteins in normal nephrogenesis, the *IRX3*<sup>-/-</sup> and *IRX5*<sup>-/-</sup> tumour cell phenotypes were in stark contrast to each other. *IRX3*<sup>-/-</sup> tumours had a shortfall of nephrogenic organisation with an extensive mesenchymal stromal element, whereas *IRX5*<sup>-/-</sup> tumours showed a differentiated nephrogenic pattern. Thus, our data strongly pointed to a differentiation-promoting role for *IRX3* in Wilms tumour and a role for *IRX5* in maintaining a pool of cells with the proliferative features of the early metanephric mesenchyme in the Wit49 xenograft system. A similar role in primary Wilms tumour material would fit well with the fact that we detected *IRX5* protein expression not only in tumour tubules but also in blastema and tumour stroma. However, the role of *IRX3* in neoplasia is likely contextual as *IRX3* rather blocks differentiation in acute leukaemia [37] and shows tumour-promoting potential in hepatocellular carcinoma [38].

An earlier study on a small sample set of Wilms tumours indicated that low mRNA expression of both *IRX3* and *IRX5* correlates to poor prognosis in Wilms tumour [6]. However, in the present study, loss of *IRX5* resulted in small, well-differentiated tumours, which suggests an oncogenic-like role for *IRX5* in Wilms tumour, well in accordance with a recently proposed role as an oncogenic driver in prostate and colorectal cancer [39–41]. One plausible explanation for the seemingly contradictory role of *IRX5* as a promotor of tumorigenesis on the one hand and the correlation of poor prognosis to its reduced mRNA expression on the other hand is its correlated expression with *IRX3* in clinical material. In a situation where both genes are downregulated, it is feasible that the lack of differentiation caused by reduced *IRX3* expression overrides the anti-tumorigenic effects of reduced *IRX5*. What drives the expression of *IRX5* in a Wilms tumour setting needs further investigation.

Our finding that *IRX3* and *IRX5* have central roles in nephrogenic differentiation highlights new possibilities to overcome the differentiation block that underlies Wilms tumour formation. The results presented here suggest that either the promotion of *IRX3* signalling or inhibition of *IRX5* signalling could be routes towards enforced differentiation in Wilms tumours. Disturbed Hippo signalling can cause nephron progenitors to differentiate into myofibroblasts [42], and stromal–epithelial communication can act via Hippo signalling components, such as *Fat4*, *Fat3* and *Dchs1/2*, to regulate kidney progenitor cell differentiation [43–45]. Thus, the bulky mesenchymal/stromal compartment of *IRX3*<sup>-/-</sup> xenograft tumours could be partly due to a low Hippo signalling activity compared to *IRX5*<sup>-/-</sup> tumours. A feasible way of targeting *IRX3* or *IRX5* is by indirect intervention with either WNT or Hippo signalling or both (reviewed in [28,46]).

WNT5A is involved in an alternative WNT pathway that is integrated with Hippo signalling [35]. At the same time, it is known that WNT5A acts to suppress tumour formation in several cancer types [36,47,48]. In colon cancer, it even induces differentiation of neoplastic cells [36]. A previous study showed that *WNT5A* is downregulated in Wilms tumour [49]. We specifically found lower WNT5A protein expression in stroma surrounding tumour tubules in *IRX3*<sup>-/-</sup> and wild-type Wit49 cells compared to *IRX5*<sup>-/-</sup> cells, suggesting that it has a role in the induction of tubulogenesis in Wilms tumours. During organ development, *Wnt5a* is often secreted and directs PCP-dependent cellular migration and patterning along concentration gradients [50]. In our material, *IRX3* and WNT5A both exhibited the strongest IHC staining levels in maturing epithelial elements. This implies a concentration gradient based on diffusion from epithelial structures into the surrounding stroma and CM. Diffused WNT5A could then promote epithelial differentiation via, for instance, *ALCAM*, in turn leading to secondary endogenous WNT5A production through autocrine-positive feedback [33]. An alternative explanation would be that WNT5A is negatively regulated by *IRX5*. However, this would be at odds with the coexistence of these two proteins in maturing renal tubules.

In summary, our data uniformly suggest a key role for *IRX3* and *IRX5* in mammalian nephrogenesis and Wilms tumour differentiation. We also find evidence for an important interplay between *IRX3* and WNT5A in driving tubular maturation as summarised in Figure 6I. This renders WNT5A a potential treatment agent for the enforced differentiation of Wilms tumours.

## Acknowledgements

This study was supported by grants from the Swedish Research Foundation, the Swedish Cancer Society, the Swedish Childhood Cancer Foundation, the Crafoord Foundation, the Royal Physiographic Society and the Medical Faculty of Lund University Sweden. The authors also acknowledge support from BioCARE, Sweden. Lund University Bioimaging Center (LBIC), Lund University and the Whole transcriptome RNA-sequencing, National Genomics Infrastructure and SciLife Uppsala core facility, Sweden are gratefully acknowledged for providing experimental resources.

## Author contributions statement

LHM conceptualised the study, wrote the original draft and administered the project. LHM, JK, DB, JE, CJ, KL, SH, CH and SLM carried out and advanced methodology. LHM, SLM, JK and DG performed formal analysis. DG, LHM, JE, SLM, HY, KL and CJ carried out the investigation. DG, KL, SH, CH, DB and JE provided resources. DG, LHM and JK critically reviewed and edited the manuscript. LHM and DG supervised the

study and acquired funding. All authors were involved in writing the paper and had final approval of the submitted and published versions.

## References

- Schedl A. Renal abnormalities and their developmental origin. *Nat Rev Genet* 2007; **8**: 791–802.
- Vujanic GM, Sandstedt B. The pathology of Wilms' tumour (nephroblastoma): the International Society of Paediatric Oncology approach. *J Clin Pathol* 2010; **63**: 102–109.
- Kaste SC, Dome JS, Babyn PS, *et al.* Wilms tumour: prognostic factors, staging, therapy and late effects. *Pediatr Radiol* 2008; **38**: 2–17.
- Pritchard-Jones K. Controversies and advances in the management of Wilms' tumour. *Arch Dis Child* 2002; **87**: 241–244.
- Grundy PE, Breslow NE, Li S, *et al.* Loss of heterozygosity for chromosomes 1p and 16q is an adverse prognostic factor in favorable-histology Wilms tumor: a report from the National Wilms Tumor Study Group. *J Clin Oncol* 2005; **23**: 7312–7321.
- Mengelbier LH, Karlsson J, Lindgren D, *et al.* Deletions of 16q in Wilms tumors localize to blastemal-anaplastic cells and are associated with reduced expression of the IRXB renal tubulogenesis gene cluster. *Am J Pathol* 2010; **177**: 2609–2621.
- Bosse A, Zulch A, Becker MB, *et al.* Identification of the vertebrate Iroquois homeobox gene family with overlapping expression during early development of the nervous system. *Mech Dev* 1997; **69**: 169–181.
- Gaborit N, Sakuma R, Wylie JN, *et al.* Cooperative and antagonistic roles for Irx3 and Irx5 in cardiac morphogenesis and postnatal physiology. *Development* 2012; **139**: 4007–4019.
- Gomez-Skarmeta JL, Modolell J. Iroquois genes: genomic organization and function in vertebrate neural development. *Curr Opin Genet Dev* 2002; **12**: 403–408.
- Bonnard C, Strobl AC, Shboul M, *et al.* Mutations in IRX5 impair craniofacial development and germ cell migration via SDF1. *Nat Genet* 2012; **44**: 709–713.
- Li D, Sakuma R, Vakili NA, *et al.* Formation of proximal and anterior limb skeleton requires early function of Irx3 and Irx5 and is negatively regulated by Shh signaling. *Dev Cell* 2014; **29**: 233–240.
- Houweling AC, Dildrop R, Peters T, *et al.* Gene and cluster-specific expression of the Iroquois family members during mouse development. *Mech Dev* 2001; **107**: 169–174.
- Marra AN, Wingert RA. Roles of Iroquois transcription factors in kidney development. *Cell Dev Biol* 2014; **3**: 1000131.
- Reggiani L, Raciti D, Airik R, *et al.* The prepattern transcription factor Irx3 directs nephron segment identity. *Genes Dev* 2007; **21**: 2358–2370.
- Alarcon P, Rodriguez-Seguel E, Fernandez-Gonzalez A, *et al.* A dual requirement for Iroquois genes during *Xenopus* kidney development. *Development* 2008; **135**: 3197–3207.
- Wingert RA, Davidson AJ. Zebrafish nephrogenesis involves dynamic spatiotemporal expression changes in renal progenitors and essential signals from retinoic acid and irx3b. *Dev Dyn* 2011; **240**: 2011–2027.
- Alami J, Williams BR, Yeger H. Derivation and characterization of a Wilms' tumour cell line, WiT 49. *Int J Cancer* 2003; **107**: 365–374.
- Gisselsson D, Lindgren D, Mengelbier LH, *et al.* Genetic bottlenecks and the hazardous game of population reduction in cell line based research. *Exp Cell Res* 2010; **316**: 3379–3386.
- Mengelbier LH, Bexell D, Shchic D, *et al.* Orthotopic Wilms tumor xenografts derived from cell lines reflect limited aspects of tumor morphology and clinical characteristics. *Pediatr Blood Cancer* 2014; **61**: 1949–1954.
- Braekeveldt N, Wigerup C, Gisselsson D, *et al.* Neuroblastoma patient-derived orthotopic xenografts retain metastatic patterns and geno- and phenotypes of patient tumours. *Int J Cancer* 2015; **136**: E252–E261.
- Shchic D, Ciornei CD, Gisselsson D. Evaluation of CITED1, SIX1, and CD56 protein expression for identification of blastemal elements in Wilms tumor. *Am J Clin Pathol* 2014; **141**: 828–833.
- Mootha VK, Lindgren CM, Eriksson KF, *et al.* PGC-1 $\alpha$ -responsive genes involved in oxidative phosphorylation are coordinately downregulated in human diabetes. *Nat Genet* 2003; **34**: 267–273.
- Subramanian A, Tamayo P, Mootha VK, *et al.* Gene set enrichment analysis: a knowledge-based approach for interpreting genome-wide expression profiles. *Proc Natl Acad Sci U S A* 2005; **102**: 15545–15550.
- Zhang SS, Kim KH, Rosen A, *et al.* Iroquois homeobox gene 3 establishes fast conduction in the cardiac His-Purkinje network. *Proc Natl Acad Sci U S A* 2011; **108**: 13576–13581.
- Bielen A, Box G, Perryman L, *et al.* Dependence of Wilms tumor cells on signaling through insulin-like growth factor 1 in an orthotopic xenograft model targetable by specific receptor inhibition. *Proc Natl Acad Sci U S A* 2012; **109**: E1267–E1276.
- Li MH, Yamase H, Ferrer F. Characterization of a WiT49 cell line derived orthotopic model of Wilms tumor. *Pediatr Blood Cancer* 2010; **54**: 316–318.
- Karlsson J, Holmquist Mengelbier L, Ciornei CD, *et al.* Clear cell sarcoma of the kidney demonstrates an embryonic signature indicative of a primitive nephrogenic origin. *Genes Chromosomes Cancer* 2014; **53**: 381–391.
- Bernascone I, Martin-Belmonte F. Crossroads of Wnt and Hippo in epithelial tissues. *Trends Cell Biol* 2013; **23**: 380–389.
- Huang L, Xiao A, Choi SY, *et al.* Wnt5a is necessary for normal kidney development in zebrafish and mice. *Nephron Exp Nephrol* 2014; **128**: 80–88.
- Dijksterhuis JP, Petersen J, Schulte G. WNT/frizzled signalling: receptor-ligand selectivity with focus on FZD-G protein signalling and its physiological relevance: IUPHAR review 3. *Br J Pharmacol* 2014; **17**: 1195–1209.
- Kikuchi A, Yamamoto H, Sato A. Selective activation mechanisms of Wnt signaling pathways. *Trends Cell Biol* 2009; **19**: 119–129.
- Carroll TJ, Das A. Planar cell polarity in kidney development and disease. *Organogenesis* 2011; **7**: 180–190.
- Cizelsky W, Tata A, Kuhl M, *et al.* The Wnt/JNK signaling target gene *alcam* is required for embryonic kidney development. *Development* 2014; **141**: 2064–2074.
- Wong JS, Meliambro K, Ray J, *et al.* Hippo signaling in the kidney: the good and the bad. *Am J Physiol Renal Physiol* 2016; **311**: F241–F248.
- Park HW, Kim YC, Yu B, *et al.* Alternative Wnt signaling activates YAP/TAZ. *Cell* 2015; **162**: 780–794.
- Mehdawi LM, Prasad CP, Ehrnstrom R, *et al.* Non-canonical WNT5A signaling up-regulates the expression of the tumor suppressor 15-PGDH and induces differentiation of colon cancer cells. *Mol Oncol* 2016; **10**: 1415–1429.
- Somerville TDD, Simeoni F, Chadwick JA, *et al.* Derepression of the Iroquois homeodomain transcription factor gene IRX3 confers differentiation block in acute leukemia. *Cell Rep* 2018; **22**: 638–652.
- Wang P, Zhuang C, Huang D, *et al.* Downregulation of miR-377 contributes to IRX3 deregulation in hepatocellular carcinoma. *Oncol Rep* 2016; **36**: 247–252.
- Myrthue A, Rademacher BL, Pittsenbarger J, *et al.* The Iroquois homeobox gene 5 is regulated by 1,25-dihydroxyvitamin D3 in human prostate cancer and regulates apoptosis and the cell

- cycle in LNCaP prostate cancer cells. *Clin Cancer Res* 2008; **14**: 3562–3570.
40. Liu T, Zhang X, Yang YM, *et al*. Increased expression of the long noncoding RNA CRNDE-h indicates a poor prognosis in colorectal cancer, and is positively correlated with IRX5 mRNA expression. *Onco Targets Ther* 2016; **9**: 1437–1448.
  41. Mori K, Nakamura H, Kurooka H, *et al*. Id2 determines intestinal identity through repression of the foregut transcription factor, Irx5. *Mol Cell Biol* 2018. <https://doi.org/10.1128/MCB.00250>–17.
  42. McNeill H, Reginensi A. Lats1/2 regulate yap/Taz to control nephron progenitor epithelialization and inhibit myofibroblast formation. *J Am Soc Nephrol* 2017; **28**: 852–861.
  43. Das A, Tanigawa S, Karner CM, *et al*. Stromal-epithelial crosstalk regulates kidney progenitor cell differentiation. *Nat Cell Biol* 2013; **15**: 1035–1044.
  44. Bagherie-Lachidan M, Reginensi A, Pan Q, *et al*. Stromal Fat4 acts non-autonomously with Dchs1/2 to restrict the nephron progenitor pool. *Development (Cambridge, England)* 2015; **142**: 2564–2573.
  45. Mao Y, Francis-West P, Irvine KD. Fat4/Dchs1 signaling between stromal and cap mesenchyme cells influences nephrogenesis and ureteric bud branching. *Development* 2015; **142**: 2574–2585.
  46. McNeill H, Woodgett JR. When pathways collide: collaboration and connivance among signalling proteins in development. *Nat Rev Mol Cell Biol* 2010; **11**: 404–413.
  47. Canesin G, Evans-Axelsson S, Hellsten R, *et al*. Treatment with the WNT5A-mimicking peptide Foxy-5 effectively reduces the metastatic spread of WNT5A-low prostate cancer cells in an orthotopic mouse model. *PLoS One* 2017; **12**: e0184418.
  48. Prasad CP, Chaurasiya SK, Guilmain W, *et al*. WNT5A signaling impairs breast cancer cell migration and invasion via mechanisms independent of the epithelial-mesenchymal transition. *J Exp Clin Cancer Res* 2016; **35**: 144.
  49. Tamimi Y, Ekuere U, Laughton N, *et al*. WNT5A is regulated by PAX2 and may be involved in blastemal predominant Wilms tumorigenesis. *Neoplasia* 2008; **10**: 1470–1480.
  50. Gao B, Song H, Bishop K, *et al*. Wnt signaling gradients establish planar cell polarity by inducing Vangl2 phosphorylation through Ror2. *Dev Cell* 2011; **20**: 163–176.
  - \*51. Gaj T, Guo J, Kato Y, *et al*. Targeted gene knockout by direct delivery of zinc-finger nuclease proteins. *Nat Methods* 2012; **9**: 805–807.
  - \*52. Cong L, Ran FA, Cox D, *et al*. Multiplex genome engineering using CRISPR/Cas systems. *Science* 2013; **339**: 819–823.
- \*Cited only in supplementary material.

## SUPPLEMENTARY MATERIAL ONLINE

### Supplementary materials and methods

#### Supplementary figure legends

**Figure S1.** Haematoxylin eosin, p53, WT1 and nuclear morphology as guidelines for xenograft tumour demarcation and tubules

**Figure S2.** Extended IRX3 and IRX5 immunostaining

**Figure S3.** Identification of *IRX3* and *IRX5* ko WiT49 cell lines

**Figure S4.** *IRX3* and *IRX5* ko Wilms tumour cells have contrasting phenotypes

**Figure S5.** Cell proliferation is reduced in *IRX5*<sup>-/-</sup> cells

**Figure S6.** Minimal stromal and excessive epithelial elements in *IRX5*<sup>-/-</sup> tumours

**Figure S7.** Different prevalence of WNT5A-positive stroma cells in *IRX3*<sup>-/-</sup> and *IRX5*<sup>-/-</sup> tumours

**Figure S8.** Tumour tubules of Wilms tumours show WNT5A positivity

**Table S1.** Clinical Wilms tumour samples

**Table S2.** IRX3 and IRX5 WiT49 knock out clones

**Table S3.** Orthotopic xenograft tumours

**Table S4.** Immunohistochemistry reagent and antibody information

**Table S5.** Gene expression data

**Table S6.** Gene set enrichment analyses

**Table S7.** Nephrogenesis, WNT- and Hippo signalling related genes